arXiv:cond-mat/0104189v1 [cond-mat.mtrl-sci] 11 Apr 2001

Electronic properties and Fermi surface of Ag(111) films deposited onto H-passivated Si(111)-(1x1) surfaces

A. Arranz
LURE, Centre Universitaire Paris-Sud, Bat. 209 D, B.P. 34, 91898 Orsay Cedex, France
and Dpt. Física Aplicada, Fac. de Ciencias, C-XII, Univ. Autónoma de Madrid, Cantoblanco, 28049 Madrid, Spain

J.F. Sánchez-Royo
LURE, Centre Universitaire Paris-Sud, Bat. 209 D, B.P. 34, 91898 Orsay Cedex, France
and Dpt. Física Aplicada, ICMUV, Univ. de Valencia, c/Dr. Moliner 50, 46100 Burjassot, Valencia, Spain

J. Avila
LURE, Centre Universitaire Paris-Sud, Bat. 209 D, B.P. 34, 91898 Orsay Cedex, France
and Instituto de Ciencia de Materiales de Madrid, CSIC, Cantoblanco, 28049 Madrid, Spain

V. Pérez-Dieste and P. Dumas
LURE, Centre Universitaire Paris-Sud, Bat. 209 D, B.P. 34, 91898 Orsay Cedex, France

M.C. Asensio*
LURE, Centre Universitaire Paris-Sud, Bat. 209 D, B.P. 34, 91898 Orsay Cedex, France
and Instituto de Ciencia de Materiales de Madrid, CSIC, Cantoblanco, 28049 Madrid, Spain
(February 1, 2008)

Silver films were deposited at room temperature onto H-passivated Si(111) surfaces. Their electronic properties have been analyzed by angle-resolved photoelectron spectroscopy. Submonolayer films were semiconducting and the onset of metallization was found at a Ag coverage of ∼0.6 monolayers. Two surface states were observed at $\overline{\Gamma}$-point in the metallic films, with binding energies of 0.1 and 0.35 eV. By measurements of photoelectron angular distribution at the Fermi level in these films, a cross-sectional cut of the Fermi surface was obtained. The Fermi vector determined along different symmetry directions and the photoelectron lifetime of states at the Fermi level are quite close to those expected for Ag single crystal. In spite of this concordance, the Fermi surface reflects a sixfold symmetry rather than the threefold symmetry of Ag single crystal. This behavior was attributed to the fact that these Ag films are composed by two domains rotated 60^o.

PACS numbers: 73.20.-r, 71.18.+y, 79.60.-i

I. INTRODUCTION

Among other metal-silicon systems, the growth of silver (Ag) onto Si(111) surfaces is one of the most extensively studied.[1] Typically, Si(111) surfaces exhibit a wide variety of reconstructions, originated by the tendency to saturate the dangling bonds resulting from the abrupt surface termination. Because of this, deposition of Ag adatoms onto these surface reconstructions results in Ag/Si(111) interfaces with strongly different electronic properties of the interface. By far, the most commonly analyzed Ag/Si(111) systems are those of Ag films onto Si(111)-(7x7) and the Ag-derived Si(111)-($\sqrt{3}$x$\sqrt{3}$)R30^o surface reconstruction. The interest in such systems lies on the preparation of well ordered structures which show new applications in optoelectronics as magnetic or optical devices. In general, it is highly desirable to achieve sharp interfaces, in which the conductivity and transport properties depend on their size and spatial distributions. Nevertheless, because of stress effects, the most common growth mode at room temperature (RT) for non-reactive Ag/Si(111) interfaces is the formation of three-dimensional islands with widely varying heights.[2–5] In order to avoid these effects and to improve the conductivity and transport properties of the Ag films, recent studies have focused their efforts on alternative growth modes and regimes.[6–8]

In this context, much effort has been devoted to find mechanisms that neutralize dangling bonds at the Si(111) surface.[9,10] With this purpose, interest has been recently revived by the obtention of artificially produced H-terminated surfaces with a high degree of homogeneity. The hydrogenation of the Si(111)-(7x7) restores the (1x1) symmetry of the bulk and seems to destroy the Fermi level (E_F) pinning of the non-hydrogenated surface.[11,12] The development of both the wet chemical treatment and the atomic hydrogen-based method has allowed the preparation of a stable and unreconstructed flat Si(111) surface,[13,14] with a nearly-defect-free termination. As a consequence of the high-quality of this hydrogenated surface, four remarkably sharp features have been recently resolved by angle-resolved photoelectron spectroscopy (ARPES), which appear to be mostly located around the $\overline{K}$-point.[14–16] The origin of these fea-

tures is attributed to: (i) A surface resonance, with a p_x-p_y symmetry,[16] (ii) A surface state identified as a Si-Si backbond state,[16] and (iii) two higher binding-energy H-Si surface states.[16,17]

In spite of the extensive investigations of the electronic properties of Ag films deposited onto clean Si(111) substrates, there remains a lack of studies on the electronic properties of Ag films deposited onto H/Si(111)-(1x1) substrates. The study of the Ag films deposited onto these surfaces has been mostly approached through structural methods,[18–20] in order to elucidate their growth mode on these passivated surfaces. Growth mode and structure of these Ag films is drastically changed by the hydrogen termination of the Si(111)-(7x7) surface.[18,19] It is well-known that Ag films deposited onto clean Si(111) surfaces grow in quasi-layer-by-layer fashion up to few monolayers (MLs) at RT, with a two-domains Ag-islands distribution.[21] At high substrate temperatures, growth of Ag films onto clean Si substrates proceeds in the Stranski-Krastanov mode.[2] Opposite to this behavior, impact-collision ion-scattering spectroscopy showed that growth of Ag films deposited onto H/Si(111)-(1x1) surfaces follows a quasi-layer-by-layer mode even at temperatures of 300 ^{o}C.[18] In this case, the forming Ag islands appeared to be thinner than those deposited onto the high-temperature clean substrates.[18,19] Moreover, it was observed that Ag films deposited onto H/Si(111)-(1x1) substrates at 300 ^{o}C tend to follow a mono-domain island distribution.[18]

With regard to the presence of H at the interface, it has been shown that its presence gradually decreases with the Ag deposition even at RT,[22,23] indicating a partial replacement of H by Ag atoms. This effect has been recently confirmed by resonant nuclear analysis of the Ag-H/Si(111) interface in 1 ML passivated Si substrates prepared by dosing atomic H at 820 K.[24] These results show that low-temperature deposition of Ag causes part of the H-monolayer migrates to the surface and the rest remaining at the interface. In contrast, deposition at 360 K prevents the presence of H at the metal surface.

In this work we report on the electronic properties of Ag films deposited onto H/Si(111)-(1x1) surfaces at RT, determined by ARPES. In Sect. II we describe the experimental setup. The results obtained by ARPES are showed and discussed in Sect. III. In this section we illustrate and discuss the evolution of the Ag valence-band structure as the film thickness increases and the influence of H on it. We finish this section with the analysis of the Fermi surface (FS) of the metallic films prepared.

II. EXPERIMENT

The experiments were performed at LURE (Orsay, France) using the French-Spanish (PES2) experimental station of the Super-Aco storage ring, described elsewhere.[25] The measurements were carried out in a purpose-built ultra-high vacuum system, with a base pressure of $5x10^{-11}$ mbar, equipped with an angle resolving 50 mm hemispherical VSW analyzer coupled on a goniometer inside the chamber. The manipulator was mounted in a two-axes goniometer that allows rotation of the sample in: (i) The whole 360^o azimuthal angle (ϕ) and (ii) In the 180^o polar emission angle relative to surface normal (θ_{off}), with an overall angular resolution of 0.5^o. The energy range of light was of 18-150 eV. Photoelectrons were excited with p-polarized synchrotron radiation, that is, with the polarization vector of incident light, the surface normal, and the emitted electrons lying in the same plane. The current incident angle of the light (Θ_i) was Θ_i=45^o. Nevertheless, some experiments were carried out as a function of Θ_i.

With this set-up, the procedure to determine the FS using ARPES is direct. For a given experiment, the photon energy ($h\upsilon$) was fixed and the intensity at the E_F was recorded, along a series of azimuthal scans, for each step of the crystal rotation about its surface normal. This procedure was repeated at different polar angle positions of the analyzer, which allows us to scan a sheet of the Brillouin zone (BZ) for each hυ. In order to measure the FS contour at different perpendicular wave vectors, the above procedure can be carried out at different photon energies. In our measurements, the typical polar intervals were 1.5^o and the azimuthal angle range was fixed at 180^o. In these conditions, the typical measuring time was between 4 and 6 hours, depending on statistics and optimal signal-to-noise ratio.

The substrates were n-doped Si(111) single crystal, with a nominal resistivity of 100 Ωcm. They were prepared *ex situ* using a wet chemical treatment that results in a passivated H/Si(111)-(1x1) surface.[13] After introducing the substrates in the chamber, the quality of the surfaces was checked out through the sharpness of the features appearing in the valence-band photoemission-spectra at $\overline{K}$-point, which are attributed to intrinsic H-Si surface states.[15,16] Ag was evaporated onto the surface at RT. The rate of evaporation, 0.06 ML/min, was determined by using a quartz microbalance. In these conditions, Ag films of thickness ranging from 0.03 to 8 ML were deposited onto H/Si(111)-(1x1) surfaces at RT.

III. RESULTS AND DISCUSSION

A. Metallization of Ag films deposited on H/Si(111)-(1x1) surfaces

Ag films were deposited at RT onto H/Si(111)-(1x1) surfaces with a nominal Ag coverage (θ_{Ag}) lower than 1 ML. Valence-band photoemission measurements were carried out in these films. Figure 1 shows the energy distribution curves (EDCs) measured in these films with hυ=32 eV at $\overline{K}$ and $\overline{\Gamma}$-points of the Si(111) surface Brillouin zone (SBZ). All the spectra are referred, in binding

energy, to the E_F. With regard to the spectra corresponding to clean substrate, the most remarkable features at $\overline{K}$-point are those appearing with binding energies between 4 and 10 eV (Fig. 1(a)). These features have been related with emission from surface states ((a), (a'), and (b') features) and a surface resonance ((b)-feature).[15,16] Opposite to this, main emission from the substrate at $\overline{\Gamma}$-point is related to bulk Si transitions.

As the θ_{Ag} increases, the substrate features at both $\overline{K}$ and $\overline{\Gamma}$-points tend to be attenuated by the film signal. This effect is expected to be stronger for surface states than for bulk-derived states or surface resonances, due to the intrinsic localization of the surface states.[16] This would explain the faster decrease of intensity of (a) and (a') features compared to that of the (b)-feature with θ_{Ag} (Fig. 1(a)), which would support the assignment of the (b)-feature as a surface resonance state.[16]

In spite of Ag deposition, non-appreciable changes in binding energy and line width of the substrate-derived features are detected as the θ_{Ag} increases. On the other side, no trace from Ag-induced surface states at these points of the SBZ were detected. These facts suggest that this metal-semiconductor interface shows a nearly abrupt and nonreactive behavior.

The insets of Fig. 1 show in detail the evolution with θ_{Ag} of the density of states (DOS) at the E_F in these submonolayer Ag films. At $\overline{\Gamma}$-point (Fig. 1(b)), the DOS at the E_F is negligible and the small emission observed can be attributed to secondary electrons. The only emission expected to appear close to the E_F at $\overline{\Gamma}$-point in metallic Ag(111) films would come from the Shockley Ag(111) surface state. In Ag films deposited onto clean Si substrates, emission from this state appears in films thicker than 3 MLs.[26] Therefore, the lack of emission at $\overline{\Gamma}$-point with hυ=32 eV is not really surprising in such nonreactive interfaces. At $\overline{K}$-point, the situation is completely different from that observed at $\overline{\Gamma}$-point. This symmetry point has a parallel wave vector ($k_\parallel$) of $k_\parallel$=1.09 Å^{-1}, which appears to be slightly smaller than the Fermi vector (k_F) of the bulk Ag(111) FS cut with hυ=32 eV along the $\overline{\Gamma K}$ direction (k_F=1.13 Å^{-1}).[27] Therefore, the evolution of the DOS at the E_F at this symmetry point is directly related with the metallization process in these films due to the *sp*-band crossing the E_F. The inset of Fig. 1(a) elucidates this point. It can be observed that the DOS at the E_F increases with the θ_{Ag} with an incipient *sp*-derived state close to the E_F at θ_{Ag}=0.56 ML. This can be considered the onset of metallization of Ag films deposited onto H/Si(111)-(1x1) surfaces. These results would confirm the nonreactive behavior of Ag overlayers and suggest that metallization process of Ag films prepared onto H/Si(111)-(1x1) surfaces at RT follows the tendency through bulk-like metallic films in a similar way to that observed in Ag films prepared onto clean Si surfaces at RT,[26] without additional metal-semiconductor surface states induced at the E_F.

As it is expected for a quasi-layer-by-layer growth of Ag films onto H/Si(111)-(1x1) substrates at RT,[18] the whole metallization process can be monotonously followed in films thicker than 1 ML. Figure 2 shows, in a similar way, the EDCs measured in films thicker than 1 ML. The main features observed in these spectra at both symmetry points correspond to the Ag *4d* valence band, appearing at binding energies higher than 4 eV. The Ag *4d* features are better resolved than those measured in Ag films with similar thickness as-deposited onto clean Si substrates. This fact can be related to the different growth mode of these films, which is an indicative of the structural improvement obtained in films prepared onto H/Si(111)-(1x1) surfaces at RT. The insets of Fig. 2 show the evolution of the DOS at the E_F with θ_{Ag}. At $\overline{K}$-point, the gradual increasing of emission at the E_F observed in the submonolayer films defines in a clear peak. At θ_{Ag}=2.4 ML, the bulk-like long lifetime *sp*-band is formed and, consequently, the metallic behavior of these Ag films is completely established at this Ag coverage. At $\overline{\Gamma}$-point, the evolution of the DOS at the E_F is completely different from that observed in the submonolayer films. In addition, Ag films of round to 2 ML show a new incipient emission in the vicinity of the E_F that becomes resolved in thicker films as two features, labelled as SS1 and SS2. These features correspond to occupied states SS1 and SS2 with binding energies of 0.10 eV and 0.35 eV, respectively. The origin of these two features will be discussed in the next section.

B. Surface states of metallic Ag films

In the previous section, it was pointed out the existence of SS1 and SS2 features in the valence band spectra at $\overline{\Gamma}$-point of Ag films deposited at RT onto H/Si(111)-(1x1) with θ_{Ag} >2 ML. Now, we discuss the origin of the states that give rise to these features. Figure 3 shows the normal-emission valence-band spectra measured with hυ=32 eV in films prepared with different conditions. In this Figure, curves *a*-*c* correspond, respectively, to 4, 5, and 6 ML-thick as-deposited Ag films. Curve *d* corresponds to the latter 6 ML-thick Ag film annealed to 300 ^{o}C for 5 min. The latter sample was annealed again to 300 ^{o}C for 15 min and then 1 ML Ag film was deposited (Curve *e*). Curve *f* corresponds to a further Ag deposition of 1 ML and then annealed to 300 ^{o}C for 5 min. The binding energies of the SS1 and SS2 states are marked by solid lines in these spectra. From these results, we can remark that: (i) These states appear with Ag deposition onto H/Si(111)-(1x1) surfaces in films thicker than 2-3 MLs and their intensities simultaneously increase with θ_{Ag}. (ii) Annealing effects make emission from the SS2 feature to decrease, whereas the SS1 feature is enhanced. Moreover, it appears that this annealing effect is irreversible with additional Ag deposition. (iii) The binding energy of the SS1 state is nearly constant in the whole Ag film-thickness range studied. Nevertheless, the SS2

feature appears slightly shifted to lower binding energy after annealing.

Figure 4 shows the valence-band spectra measured by ARPES along the [$\overline{1}$10] direction with hυ=32 eV in a 7 ML-thick Ag film deposited at RT onto H/Si(111)-(1x1) and annealed to 300 ^{o}C for 20 min. Similar results are obtained for the spectra measured along the [$\overline{2}$11] symmetry direction (not shown). Small solid bars indicate the position of the SS1 and SS2 states as they disperse. The inset shows the band diagram as extracted from the dispersion of these features. The SS1 and SS2 states appear to cross the E_F at $k_{\parallel}$=0.16 and 0.22 Å^{-1}, respectively. Solid lines are parabolic fitting curves of the obtained dispersions, which correspond to an in-plane effective mass ($m^*_{\parallel}$) of $m^*_{\parallel}$=0.88m_o and 0.56m_o for the SS1 and SS2 states, respectively, being m_o the free electron mass.

Dispersion of SS1 and SS2 states along the [111] symmetry direction has been also determined. Figure 5 shows the normal-emission valence-band spectra measured in a 6 ML-thick Ag film deposited at RT onto H/Si(111)-(1x1) and then annealed to 300 ^{o}C for 5 min, as a function of the hυ. Solid lines indicate the binding energies of the SS1 and SS2 states in these spectra. From these results, it can be observed that these states do not disperse in the perpendicular wave vector range studied, which extends over the whole ΓL symmetry direction of the Ag(111) BZ.

The facts observed are: (i) SS1 and SS2 show a parabolic in-plane dispersion (Fig. 4) and (ii) they do not disperse with hυ (Fig. 5), indicating clearly that SS1 and SS2 states can be considered as two-dimensional states. The first state (SS1) can be identified as the well-known Shockley surface state of bulk Ag(111) (or *sp*-surface state), whose existence is due to the break of crystalline periodicity at the surface.[28] This state is located in the *sp* band gap at the L-point of the bulk BZ. ARPES measurements carried out in Ag(111) single crystal show that this state disperses as a parabolic surface state centered at $\overline{\Gamma}$-point, with a maximum binding energy of ∼0.12 eV and crossing the E_F at $k_{\parallel}$=0.14 Å^{-1}.[29] On the other side, This state has been observed in Ag films deposited onto clean Si(111) and Cu(001), when these films are thicker than 2-3 MLs.[26,30] All these facts are in concordance with our observations and support the assignment of SS1 as the Ag(111) *sp*-surface state.

With regard to the two-dimensional SS2 state, it appears at 0.25 eV below the SS1 surface state. This state is rather confined in the surface and spreads along the surface. At first sight, this state may be tentatively assigned to be a Ag(111) *sp*-derived quantum-well state. Shallow quantum states with $m^*_{\parallel}$ ∼0.4m_o have been observed at binding energies of 0.5 eV,[31,32] which is, in fact, quite close the top of the Ag *sp*-band in the ΓL-direction.[32,33] Nevertheless, this assignment of the SS2 state seems not to be correct, since it is not expected quantum states at binding energies of 0.35 eV in 2ML-Ag films and this state appears slightly outside the *sp*-band range in the Ag ΓL direction. In addition, its binding energy appears to be constant with θ_{Ag} in the thickness range of the Ag films studied. In fact, a shallow Ag(111) *sp*-quantum state should show a shift of ∼0.2 eV to lower binding energies in the Ag thickness range of 4-8 MLs, following the phase-accumulation-model.[34]

After these considerations, it appears that the SS2 state is related to a Ag-derived surface state or surface resonance, since it appears quite close, in binding energy, to the bottom of the *sp*-gap of the Ag valence-band projected onto the (111)-face. From our results (Fig. 2 and Fig. 4), we have observed that SS2 emission increases in a similar way to that of SS1 as a function of the Ag deposition. In addition to this, this state appears to be a parabolic state with a $m^*_{\parallel}$ quite close to that obtained for the *sp*-surface state of bulk Ag(111).[35] These results suggest that SS2 is a surface state related to a bulk-like termination of the Ag(111) films, as the SS1 state, shifted to higher binding energy.

In order to check these assignments for both SS1 and SS2 states, we have analyzed the behavior of their wave functions as a function of Θ_i. By means of Θ_i, the weight of the components of the polarization vector of light can be tuned, either along the normal to the surface (large Θ_i) or contained in the surface plane (small Θ_i). In this way, emission from perpendicular-to-surface components of the wave function is enhanced at large Θ_i and decreased at small Θ_i. In the case that the emission plane is a mirror plane, p-polarized excitation selects even states with respect to this plane. As we are interested only in *sp*-states, even states refer to *p*-states lying in the emission plane and *s*-states. Therefore, at large Θ_i, it would be expected an enhancement of their p_z-character.

Figure 6 shows the normal-emission valence-band spectra measured with hυ=50 eV in a 6 ML-thick Ag film deposited onto H/Si(111)-(1x1) and then annealed to 300 ^{o}C for 5 min, as a function of the Θ_i. The emission plane is that determined by the $\overline{\Gamma K}$-direction, which can be considered as a mirror plane if we neglect multiple scattering effects.[16] Solid lines indicate the binding energies of the SS1 and SS2 states. As one can observe, intensity of both states increases with Θ_i. Nevertheless, the intensity from SS1 increases slower than that from the SS2. In fact, the SS1 increase is the 70% of that of SS2, as calculated after background subtraction. These results can be explained if we consider that SS1 and SS2 are bulk-induced surface states. The Ag(111) *sp*-gap is a Shockley inverted gap. In this case, *sp*-surface states inside this gap are, basically, *s*-like at the top and *p*-like at the bottom. If we assume SS1 and SS2 to be *sp*-surface states, they are expected to show a rather *p*-like behavior since they appear quite close to the bottom of the gap. Therefore, the observed increase of the SS1 and SS2 intensity with Θ_i can be attributed to their p_z-character. In any case, if they were *only* *p*-like states, they should show the same Θ_i-dependence of the intensity. Nevertheless, SS1

shows a smoother Θ_i-dependence than that of SS2 which can be attributed to a non-negligible *s*-component. This contribution would be expected to be more important for *sp*-surface states at the top of the gap, which is coherent with our results.

The behavior of the two different SS1 and SS2 features as coming from the *sp*-surface state seems to be established. The question now, is to determine the origin of the splitting of the Ag *sp*-surface state into the SS1 and SS2 features. On one side, our results show that annealing processes make an irreversible decrease of the emission from SS2, whereas that from SS1 increases (Fig. 3). On the other side, it has been observed that Ag deposited onto H/Si(111)-(1x1) surfaces at RT partially removes H from the metal-semiconductor interface and this desorption process is enhanced at higher deposition temperatures.[22–24] This behavior has been also observed in Cu and Au films deposited onto these substrates.[12,24] A similar H-desorption mechanism has also been observed when the studied films RT-deposited were annealed.[23,36] These facts suggest that the SS2 state is related to the presence of H at the metal-semiconductor interface, which somehow makes the bulk Ag(111) surface state appear closer to the *sp*-band gap edge.

Several effects can cause a shift of the *sp*-surface state. In the following, we will discuss the different possibilities for H to induce such effect. Let us now discuss the possibility of the existence of different Ag relaxed regions in films deposited onto H/Si(111) surfaces. It has been observed that the binding energy of the *sp*-surface state can differ from one substrate to other, depending on strain.[38] Nevertheless, this seems not to be the case of films as-deposited onto H/Si(111)-(1x1), where only two splitted surface states are observed. If this splitting was induced by strain, the Ag films would be mostly composed by two differently strained domains, which would imply that different points of the Ag BZ are simultaneously probed by ARPES. This fact would make that the measured bulk Ag *4d* features appeared anomalously broadened, which is not observed.

The study of the nature of surface states can be analyzed in the workframe of the phase-accumulation model,[34] based on the idea that surface states can be considered as electrons trapped between the surface gap and the surface barrier.[28] In this model, differences of the binding energy of surface states are expected via the surface-barrier and crystal phases.

In principle, there are two possibilities for H to modify the binding energy of the bulk Ag(111) surface state. The first one is related to the fact that Ag deposition at RT removes H from the interface, which seems to migrate to the metal surface.[24] This H on the surface appears to be mostly removed when films are annealed at high temperatures.[24] Under these conditions, the presence of H on the metallic surface could induce a shift of the surface state to higher binding energies (ΔSS) as far as H produced a decrease of the work-function of the metal at the surface and, consequently, a decrease of the surface-barrier phase.[34] In fact, these effects have been observed after adsorption of submonolayer alkali-metals on Cu(111) and on Ag(111) films deposited onto graphite and Si(111)-(7x7) at low temperature.[38,39] In these cases, the magnitude of the observed ΔSS was a $\sim$10-20% of the work-function decrease. Nevertheless, in contrast to the observed role of alkali metals on metallic surfaces, it has been observed that the presence of H at the Ag(111) and Ag(110) surfaces increases the metal work-function at the surface by 0.2-0.3 eV,[40,41] slightly shifting the Ag *sp*-surface state to lower binding energies. These facts suggest that the splitting of the *sp*-surface state can not be attributed to the presence of H at the metal surface.

The second possibility for H to modify the binding energy of the Ag(111) *sp*-surface state comes from the presence of absorbed H at the metal-semiconductor interface. After Ag deposition, and mostly after annealing processes, H can be progressively desorbed from the interface. Nevertheless, large H-covered areas of Si can stay underneath the Ag film, since, when one initial Ag cluster is formed, Ag adatoms appear not to be spontaneously substituted for H atoms around Ag adsorption sites.[20] This situation would induce two different limiting conditions as far as the surface-state wave-function could be influenced by surface conditions. It has been early observed that Ag *sp*-surface state shifts to lower binding energy as thicker Ag films are deposited onto 1ML-Au/Ag substrates,[42] recovering a bulk-like situation in $\sim$10ML-thick Ag films. This fact was explained by the presence of the interlayer Au film, which downshifts the bulk-like Ag surface state. It those systems, the decay length of the surface state was determined to spread along several MLs (28 Å).[42] In our case, a similar behavior may be expected in Ag films deposited onto H/Si(111)-(1x1) surfaces, where H appears to introduce a larger shift of the surface state than that observed in the Ag/1ML-Au/Ag system. This effect could be also understood in the frame of the phase-accumulation model.[34] The presence of H at the interface would be expected to increase the reflectivity of the *sp*-surface state, due to its long decay length compared to the film thickness.[42] This fact would induce an increase of the effective crystal phase and, therefore, the *sp*-surface state would downshift. In order to estimate the magnitude of this effect, an increase of the crystal phase of round to 30-40% would downshift the sp-surface state in $\sim$0.2 eV, which would reproduce quite well the behavior observed in our data for Ag films deposited onto H/Si(111)-(1x1) substrates.

C. Fermi surface

In this section we analyze the electronic properties of the Ag films beyond the metallization onset, centering this study on the determination of the FS of these films. The image in Fig. 7 shows the photoelectron angular distribution measured at the E_F with hυ=32 eV in a

6 ML Ag film deposited onto H/Si(111)-(1x1) and then annealed to 300 ^{o}C for 5 min. Photoelectron angular distribution measurements were carried out by selecting x-axis corresponding to the $[\overline{1}10]$ direction of $k_{\parallel}$. The image has been scaled in such a way that it is linear in photoemission intensity and in $k_{\parallel}$. The photoemission intensity is maximum for the brightest feature and minimum for the darkest one. In this image, well-defined features are labelled, indicating the momentum distribution, as a function of $k_{\parallel y}$ and $k_{\parallel x}$, of initial states lying at the E_F. The Ag SBZ contours are also plotted on the image, following the extended zone scheme.

In the center of the image it can be observed two different features, labelled as SS1 and SS2. The SS1 feature appears as an intense spot at the center of the image of $\sim$0.10 Å^{-1} in size, whereas the SS2 feature is a homogeneous ring-like feature centered at $\overline{\Gamma}$-point with a radius of 0.23 Å^{-1}. These features appear at the FS cut as a consequence of the crossing of the E_F of the SS1 and SS2 surface states, as these states disperse. The fact that these states show such a circular symmetry in the $k_{\parallel}$-plane indicates that these states are isotropic parabolic states, as expected for *sp*-derived surface states in bulk metallic systems.[37]

Besides to the surface-state-related features, additional ones appear in the image, at higher $k_{\parallel}$ values, which have been labelled as FS1, FS2, and FS2'. The FS1 feature appears as a distorted ringlike inside the first SBZ, which corresponds to the cut of the bulk Ag(111) FS in the first BZ.[43] From this feature, the k_F values of the FS of these Ag films can be extracted. In order to do this, one should take into account experimental energetic-window effects, which move the E_F band-crossing-point away from the maximum intensity of emitted photoelectrons at the E_F towards the unoccupied-states side.[27,44] In our experiments, the energetic window was 0.2 eV with hυ=32 eV. From this analysis, it was obtained that this Ag FS cut shows a maximum and minimum k_F values of k_F=1.29 and 1.16 Å^{-1}, which occur along the $[\overline{1}10]$ and $[\overline{2}11]$ (or $[\overline{11}2]$) directions, respectively. These values are in concordance with those obtained in metallic Ag films prepared onto Si(111)-(7x7) surfaces.[43] The resemblance between the FS of both Ag films appears not only in the k_F values as well as in the lifetime of *sp*-states at the E_F.[27] Intrinsic photoemission line width of states at the E_F is dominated by photoelectron lifetime.[45] In our experiments, the line width of the FS1 feature, where it can be isolated from other contributions, is of 0.28$\pm$0.04 Å^{-1} in average, which implies that the inverse lifetime of photoelectrons is of 4.0$\pm$0.5 eV,[27] coherently with that expected in the bulk material for photoelectrons excited with hυ=32 eV.[27,46]

The rest of features observed in Fig. 7 (FS2 and FS2') appear outside of the first SBZ, as a semi-circular feature (FS2) below a wide spot-like feature (FS2'). The presence of these features is expected from neighboring BZs, which would be measured with hυ=32 eV.[43] However, the most remarkable electronic information to be extracted from the FS of these metallic films is that it shows a sixfold symmetry, instead of the typical threefold symmetry found in the three-dimensional Ag single crystal. The loss of symmetry of the FS of these films can be related to the fact that Ag films deposited onto H/Si(111)-(1x1) at RT are composed by two domains rotated 60^o.

In order to illustrate this point, we have analyzed the influence of the two-domains character of the films on the resulting Ag(111) FS. Figure 8 shows (on the left) the band dispersion of the *sp*-band of Ag(111) single crystal along the high-symmetry directions of the SBZ: $[\overline{1}10]$ ($k_{\parallel x}$), $[\overline{2}11]$ ($k_{\parallel y}$), and $[\overline{11}2]$, as would be obtained by ARPES with hυ=32 eV.[43] In this plot, the crossing-points of the *sp*-band with the E_F are indicated, which are labelled as e_1-e_5. Each one of these points defines one point of the Ag(111) FS cut (middle plot) and, extending this to the whole BZ, a two-dimensional image of the Ag FS can be obtained. This FS cut of Ag single crystal shows the intrinsic threefold symmetry of the Ag BZ. The obtention of such a FS by ARPES assumes that each direction of the hexagonal Ag SBZ is scanned along one experimental azimuth (upper plot). Nevertheless, this seems not to be the case of the Ag films prepared onto H/Si(111)-(1x1) at RT. A film composed of two domains rotated 60^o would artificially produce, by ARPES, a 60^o-overlapping of the band structure, of the SBZ, and, therefore, of the FS (right plots in Fig. 8). Since one experimental azimuth simultaneously scans two 60^o-differing directions of the Ag SBZ, belonging each one to two different domains.

The fact that Ag films deposited onto H/Si(111)-(1x1) at RT and then annealed to 300 ^{o}C for 5 min are composed by two domains rotated 60^o has been also observed in Ag films of similar thicknesses deposited onto Si(111)-(7x7).[43] Nevertheless, in contrast to the results observed in films deposited onto H/Si(111)-(1x1) at RT, it seems that high-temperature Ag deposition favors a mono-domain growth.[22] These facts suggest that there exists an activation energy for the Ag nucleation beyond that mono-domain Ag growth is favored. In addition to this, the fact that annealing process carried out after deposition appears not to favor this structural transition seems to confirm the fact observed that Ag deposition rate may also play a role in the obtention of mono-domain films.[36] Nevertheless, much work should be done to elucidate this point. In any case, these results are promising and suggest that a good knowledge and control of the growth conditions of Ag films onto H/Si(111)-(1x1) substrates may improve the conductivity and transport properties of these films, since the influence of electronic barriers and hopping processes would be reduced.

IV. SUMMARY

Silver films of different thickness (0-8 MLs) were deposited at RT onto H-passivated Si(111) surfaces. Their electronic properties have been analyzed by ARPES, probing $\overline{K}$ and $\overline{\Gamma}$-points of the Si(111) SBZ. The valence-band spectra of submonolayer Ag films appeared to follow the evolution expected for an abrupt and nonreactive metal-semiconductor interface, with no-trace observed from Ag-induced surface states at these points of the SBZ. Bulk-like metallization process was followed by analyzing the evolution of the DOS at the E_F at Si(111) $\overline{K}$-point, which coincides, at $h\upsilon$=32 eV, with the crossing-point of the bulk Ag *sp*-band with the E_F. At initial Ag growth-stage, films appeared to be semiconducting and the onset of metallization was established at a coverage of ∼0.6 MLs. The bulk-like metallic behavior was completely defined in Ag films of 2-3 MLs and the small line width of the Ag *4d*-derived features indicates that high-quality (111)-oriented films can be prepared onto H-passivated Si surfaces.

Two well-defined Ag-derived features appeared in the valence-band spectra measured at $\overline{\Gamma}$-point, in films thicker than 2 MLs. These features, labelled as SS1 and SS2, were assigned to occupied states with binding energies of 0.1 and 0.35 eV, respectively. These states were both identified, by means of their perpendicular and parallel dispersion, as two surface states appearing at the *sp*-gap of the Ag SBZ and related to the *sp*-surface state of bulk Ag(111). As expected for such surface state, the wave function of both SS1 and SS2 states shows a pronounced *p*-like behavior, as revealed by photoemission measurements tuning the components of the polarization vector of light. The existence of two different surface states with the same origin was attributed to the non-homogeneous presence of H at the interface, due to the fact that Ag deposition and annealing process partially desorb H from the interface and, therefore, a downshift of the *sp*-surface state is produced in regions where H is still present.

The electronic properties of metallic Ag films deposited at RT onto H-passivated substrates were analyzed by measurements of photoelectron angular distribution at the E_F with $h\upsilon$=32 eV. With this technique, a cross-sectional cut of the FS of these films has been obtained with this $h\upsilon$. The k_F values of this FS cut obtained in different symmetry directions appeared to be in good agreement with those expected for bulk-like Ag(111) single crystal. A similar agreement was also found for the photoelectron lifetime of states at the E_F. In spite of the fact that the FS cut resembles a two-dimensional cut of the three-dimensional bulk-like Ag FS, it reflects a sixfold symmetry rather than the threefold symmetry expected for Ag single crystal. This indicates that these Ag films are composed by two domains rotated 60^o.

ACKNOWLEDGMENTS

This work was financed by DGICYT (Spain) (Grant No. PB-97-1199) and the Large Scale Facilities program of the EU to LURE. Financial support from the Comunidad Autónoma de Madrid (Project No. 07N/0042/98) is also acknowledged. A.A. and J.F.S.-R. acknowledge financial support from the Ministerio de Educación y Cultura of Spain.

* Electronic address: asensio@lure.u-psud.fr and mcasensio@icmm.csic.es

[1] S. Hasegawa, X. Tong, S. Takeda, N. Sato, and T. Nagao, Prog. in Surf. Sci. **60**, 89 (1999).
[2] S. Hasegawa, H. Daimon, and S. Ino, Surf. Sci. **186**, 138 (1987).
[3] K.R. Roos and M.C. Tringides, Phys. Rev. B **47**, 12705 (1993).
[4] R. Biswas, K.R. Roos, and M.C. Tringides, Phys. Rev. B **50**, 10932 (1994).
[5] Z.H. Zhang, S. Hasegawa, and S. Ino, Phys. Rev. B **55**, 9983 (1997).
[6] Y. Nakajima, G. Uchida, T. Nagao, and S. Hasegawa, Phys. Rev. B **54**, 14134 (1996).
[7] M. Henzler, T. Lüer, and A. Burdach, Phys. Rev. B **58**, 10046 (1998).
[8] X. Tong, C.S. Jiang, K. Horikoshi, and S. Hasegawa, Surf. Sci. **449**, 125 (2000).
[9] R.I.G. Uhrberg and G.V. Hansson, Crit. Rev. Solid State Mater. Sci. **17**, 133 (1991).
[10] K. Oura, V.G. Lifshits, A.A. Saranin, A.V. Zotov, and M. Katayama, Surf. Sci Rep. **35**, 1 (1999).
[11] V. Yu. Aristov, G. Le Lay, K. Hricrovini, A. Taleb-Ibrahimi, P. Dumas, R. Günther, J. Osvald, and G. Indlekofer, J. Electron Spectrosc. Relat. Phenom. **68**, 419 (1994).
[12] C. Grupp and A. Taleb-Ibrahimi, Phys. Rev. B. **57**, 6258 (1998).
[13] G.S. Higashi, Y.J. Chabal, G.W. Trucks, and K. Raghavachari, Appl. Phys. Lett. **56**, 656 (1990); G. S. Higashi, R. S. Becker, Y. J. Chabal, and A. J. Becker, Appl. Phys. Lett. **58**, 1656 (1991); P. Dumas, Y.J. Chabal, and G.S. Higashi, Phys. Rev. Lett. **65**, 1124 (1990).
[14] C.J. Karlsson, F. Owman, E. Landemark, Y.-C. Chao, P. Mårtensson, and R.I.G. Uhrberg, Phys. Rev. Lett. **72**, 4145 (1994).
[15] K. Hricovini, R. Günther, P. Thiry, A. Taleb-Ibrahimi, G. Indlekofer, J.E. Bonnet, P. Dumas, Y. Petroff, X. Blase, X. Zhu, S.G. Louie, Y.J. Chabal, and P.A. Thiry, Phys. Rev. Lett. **70**, 1992 (1993).
[16] S. Gallego, J. Avila, M. Martin, X. Blase, A. Taleb, P. Dumas, and M.C. Asensio, Phys. Rev. B **61**, 12628 (2000).
[17] X. Blase, X. Zhu, and S.G. Louie, Phys. Rev. B **49**, 4973 (1994).

[18] K. Sumitomo, T. Kobayashi, F. Shoji, K. Oura, and I. Katayama, Phys. Rev. Lett. **66**, 1193 (1991).
[19] M. Naitoh, F. Shoji, and K. Oura, Jpn. J. Appl. Phys. **31**, 4018 (1992).
[20] M. Sakurai, C. Thirstrup, and M. Aono, Phys. Rev. B **62**, 16167 (2000).
[21] K. Sumitomo, K. Tanaka, Y. Izawa, I. Katayama, F. Shoji, K. Oura, and T. Hanawa, Appl. Surf. Sci. **41-42**, 112 (1989).
[22] M. Naitoh, A. Watanabe, and S. Nishigaki, Surf. Sci. **357/358**, 140 (1996).
[23] M. Naitoh, F. Shoji, and K. Oura, Surf. Sci. **242**, 152 (1991).
[24] K. Fukutani, H. Iwai, Y. Murata, and H. Yamashita, Phys. Rev. B. **59**, 13020 (1999).
[25] J. Avila, C. Casado, M.C. Asensio, J.L. Pérez, M.C Muñoz, and F. Soria, J. Vac. Sci. Technol. A **13**, 1501 (1995).
[26] A. L. Wachs, A.P. Shapiro, T.C. Hsieh, and T.-C. Chiang, Phys. Rev. B **33**, 1460 (1986).
[27] J.F. Sánchez-Royo, J. Avila, V. Pérez-Dieste, and M.C. Asensio, Surf. Sci. (to be published).
[28] P.M. Echenique and J.B. Pendry, J. Phys. C **11**, 2065 (1978).
[29] B.A. McDougall, T. Balasubramanian, E. Jensen, Phys. Rev B **51**, 13891 (1995).
[30] J.G. Tobin, S.W. Robey, L.E. Klebanoff, and D.A. Shirley, Phys. Rev B **35**, 9056 (1987).
[31] M.A. Mueller, A. Samsavar, T. Miller, and T.-C. Chiang, Phys. Rev. B **40**, 5845 (1989); K. Takahashi, A. Tanaka, H. Sasaki, W. Gondo, S. Suzuki, and S. Sato, Phys. Rev. B **60**, 8748 (1999) ; *for a review* T.-C. Chiang, Surf . Sci. Rep. **39**, 181 (2000).
[32] M.A. Mueller, T. Miller, and T.-C. Chiang, Phys. Rev B **41**, 5214 (1990).
[33] H. Eckardt, L. Fritsche, and J. Noffke, J. Phys. F **14**, 97 (1984); G. Fuster, J.M. Tyler, N.E. Brener, J. Callaway, and D. Bagayoko, Phys. Rev. B **42**, 7322 (1990).
[34] N.V. Smith, Phys. Rev. B **32**, 3549 (1985); N.V. Smith, N.B. Brookes, Y. Chang, and P.D. Johnson, Phys. Rev. B **49**, 332 (1994).
[35] S.D. Kevan, Phys. Rev. Lett **50**, 526 (1983); Phys. Rev. B **33**, 4364 (1986); K. Takahashi, A. Tanaka, M. Hatano, H. Sasaki, S. Suzuki, and S. Sato, J. Electron Spectrosc. Relat. Phenom. **88-91**, 347 (1998) *and references therein.*
[36] A. Nishiyama, G. ter Horst, P.M. Zagwijn, G.N. Van der Hoven, J.W.M. Frenken, F. Garten, A.R. Schlatmann, and J. Vrijmoeth, Surf. Sci. **350**, 229 (1996).
[37] S. Hüfner, *Photoelectron Spectroscopy*, Springer Series in Solid-State Sciences n. **82** (Springer-Verlag, Berlin Heidelberg, 1995).
[38] G. Neuhold and K. Horn, Phys. Rev. Lett. **78**, 1327 (1997).
[39] S.Å. Lindgren and L. Walldén, Solid State Commun. **28**, 283 (1978); **34**, 671 (1980).
[40] G. Lee and E.W. Plummer, Phys. Rev. B **51**, 7250 (1995).
[41] P.T. Sprunger and E.W. Plummer, Phys. Rev. B **48**, 14436 (1993).
[42] T.C. Hsieh, T. Miller, and T.-C. Chiang, Phys. Rev. Lett. **55**, 2483 (1985).
[43] J.F. Sánchez-Royo, J. Avila, V. Pérez-Dieste, M. De Seta, and M.C. Asensio, *to be submitted.*
[44] Th. Straub, R. Claessen, P. Steiner, S. S. Hüfner, V. Eyert, K. Friemelt, and E. Bucher, Phys. Rev. B **55**, 13473 (1997).
[45] N.V. Smith, P. Thiry, Y. Petroff, Phys. Rev. B **47**, 15476 (1993).
[46] A. Goldmann, W. Altmann, and V. Dose, Solid State Comm. **79**, 511 (1991).

FIG. 1. EDCs measured with hυ=32 eV in Ag films deposited at RT onto H/Si(111)-(1x1) surfaces, at: (a) Si(111) $\overline{K}$-point and (b) $\overline{\Gamma}$-point. The corresponding Ag coverage is indicated on each curve. The different labelled features are those corresponding to the substrate. The insets show in detail the evolution with coverage of the DOS at the E_F.

FIG. 2. EDCs measured with hυ=32 eV in Ag films deposited at RT onto H/Si(111)-(1x1) surfaces, at: (a) Si(111) $\overline{K}$-point and (b) $\overline{\Gamma}$-point. The corresponding Ag coverage is indicated on each curve. Labelled features are those of Fig. 1. The insets show in detail the evolution with coverage of the DOS at the E_F. Two features, labelled as SS1 and SS2, have been identified at $\overline{\Gamma}$-point close to the E_F.

FIG. 3. Normal-emission valence-band spectra measured with hυ=32 eV in different Ag films deposited at RT onto H/Si(111)-(1x1). Curves *a*-*c* correspond, respectively, to 4, 5, and 6 ML-thick as-deposited Ag films. Curve *d* corresponds to the latter 6 ML-thick Ag film annealed to 300 ^{o}C for 5 min. Curve *e* corresponds to the latter one annealed again to 300 ^{o}C for 15 min and then 1 ML-thick Ag film was deposited. Curve *f* corresponds to a further Ag deposition of 1 ML and then annealed to 300 ^{o}C for 5 min. The binding energies of the SS1 and SS2 states are indicated by solid lines in these spectra.

FIG. 4. Valence-band spectra measured by ARPES along the [$\overline{1}$10] direction with hυ=32 eV in a 7 ML-thick Ag film deposited at RT onto H/Si(111)-(1x1) and annealed to 300 ^{o}C for 20 min. Small solid bars indicate the binding energies of the SS1 and SS2 states as they disperse. The inset shows the band diagram as extracted from the dispersion of these features. Solid lines are parabolic fitting curves of the obtained dispersions.

FIG. 5. Normal-emission valence-band spectra measured in a 6 ML-thick Ag film deposited at RT onto H/Si(111)-(1x1) and then annealed to 300 ^{o}C for 5 min, as a function of the hυ. Solid lines indicate the binding energies of the SS1 and SS2 states in these spectra.

FIG. 6. Normal-emission valence-band spectra measured with hυ=50 eV in a 6 ML-thick Ag film deposited onto H/Si(111)-(1x1) and then annealed to 300 ^{o}C for 5 min, as a function of the incident angle of light Θ_i. Solid lines indicate the binding energies of the SS1 and SS2 states.

FIG. 7. (color) Photoelectron angular distribution measured at the E_F with hυ=32 eV in a 6 ML Ag film deposited onto H/Si(111)-(1x1) and then annealed to 300 ^{o}C for 5 min. The different features observed have been labelled in the image. The hexagonal Ag(111) SBZ is plotted onto the image.

FIG. 8. On the left. Dispersion of the bulk Ag(111) *sp*-band along the $[\overline{1}10]$ ($k_{\parallel x}$), $[\overline{2}11]$ ($k_{\parallel y}$), and $[\overline{11}2]$ that would be obtained by ARPES with hυ=32 eV. The crossing-points of *sp*-band with the E_F are indicated and labelled as e_1-e_5. These points are also indicated on the corresponding Ag(111) FS cut (middle plot). The hexagonal SBZ is also plotted and high-symmetry directions are indicated (upper plot). On the right. (cross, dots) Band dispersion that would be obtained in a situation corresponding to Ag films with two domains rotated 60^o. The resulting FS cut and SBZ are also plotted.

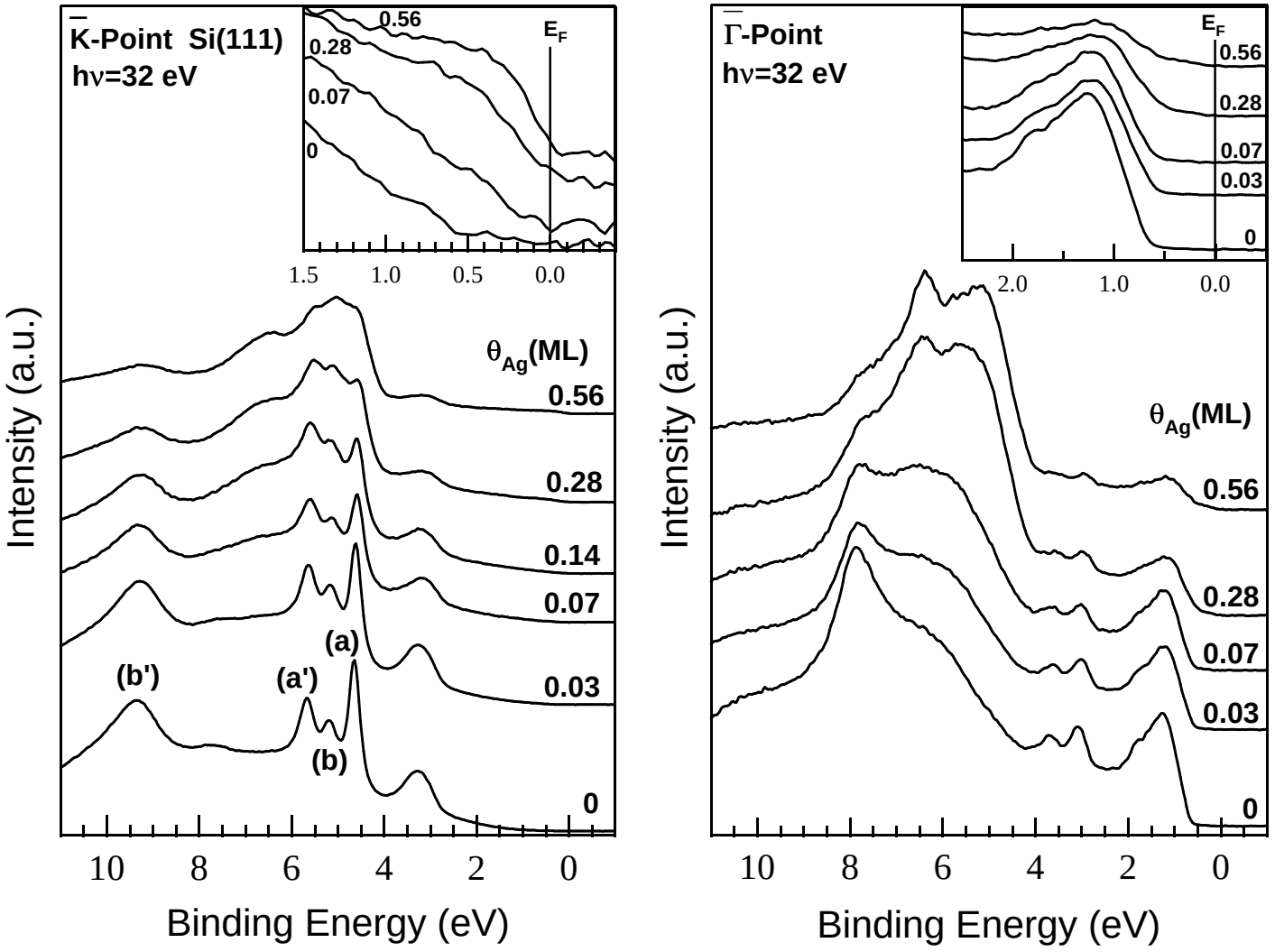
K-Point Si(111)
hν=32 eV
0.56
0.28
0.07
0
E_F
1.5
1.0
0.5
0.0
θ_Ag(ML)
0.56
0.28
0.14
0.07
0.03
0
(a)
(a')
(b)
(b')
Intensity (a.u.)
10
8
6
4
2
0
Binding Energy (eV)
Γ-Point
hν=32 eV
E_F
0.56
0.28
0.07
0.03
0
2.0
1.0
0.0
θ_Ag(ML)
0.56
0.28
0.07
0.03
0
Intensity (a.u.)
10
8
6
4
2
0
Binding Energy (eV)

(a) (b)

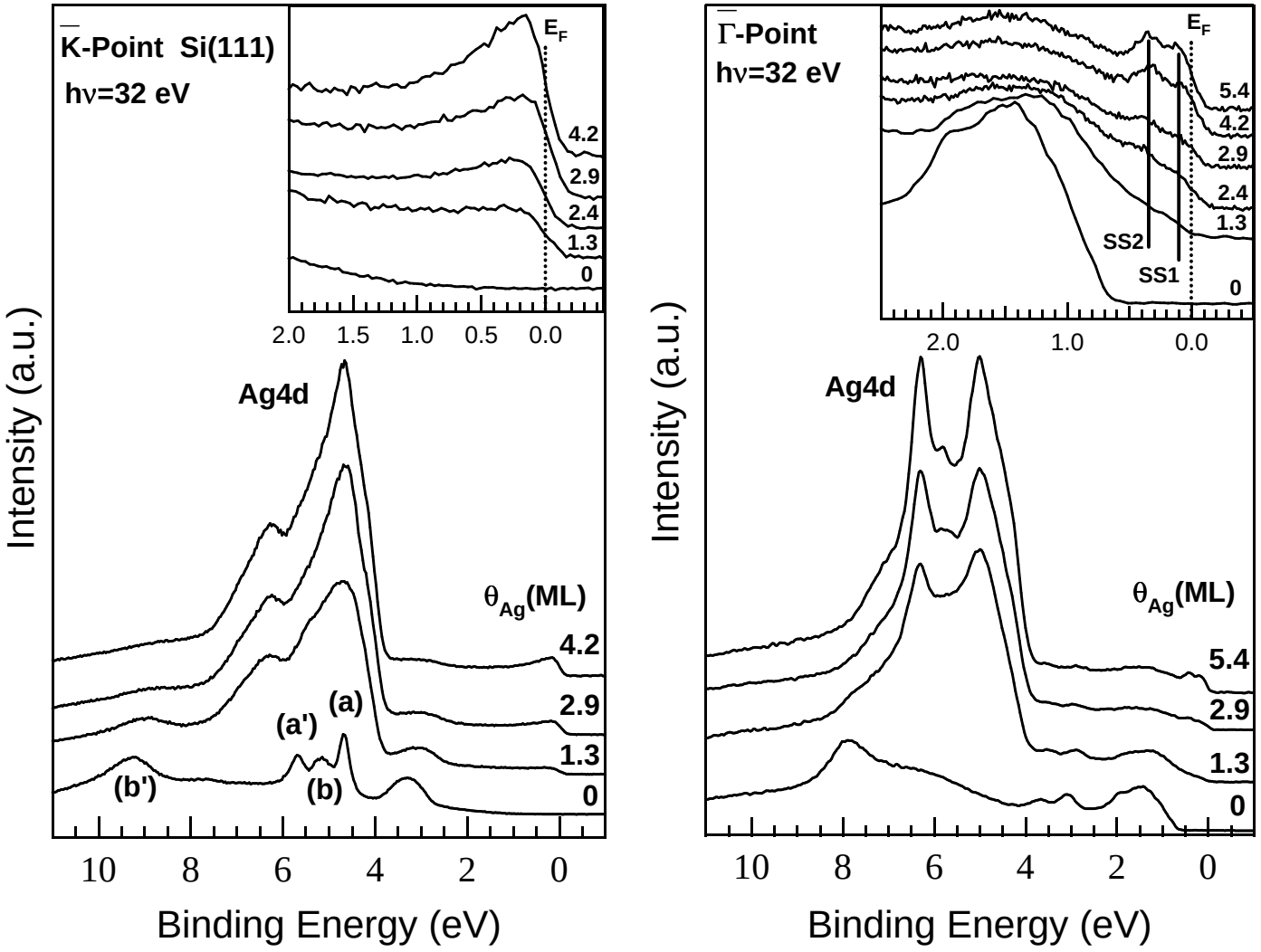
K-Point Si(111)
hν=32 eV
E_F
4.2
2.9
2.4
1.3
0
2.0 1.5 1.0 0.5 0.0
Ag4d
θ_Ag(ML)
4.2
2.9
1.3
0
(a)
(a')
(b)
(b')
Intensity (a.u.)
10 8 6 4 2 0
Binding Energy (eV)
(a)
Γ-Point
hν=32 eV
E_F
5.4
4.2
2.9
2.4
1.3
0
SS2
SS1
2.0 1.0 0.0
Ag4d
θ_Ag(ML)
5.4
2.9
1.3
0
Intensity (a.u.)
10 8 6 4 2 0
Binding Energy (eV)
(b)

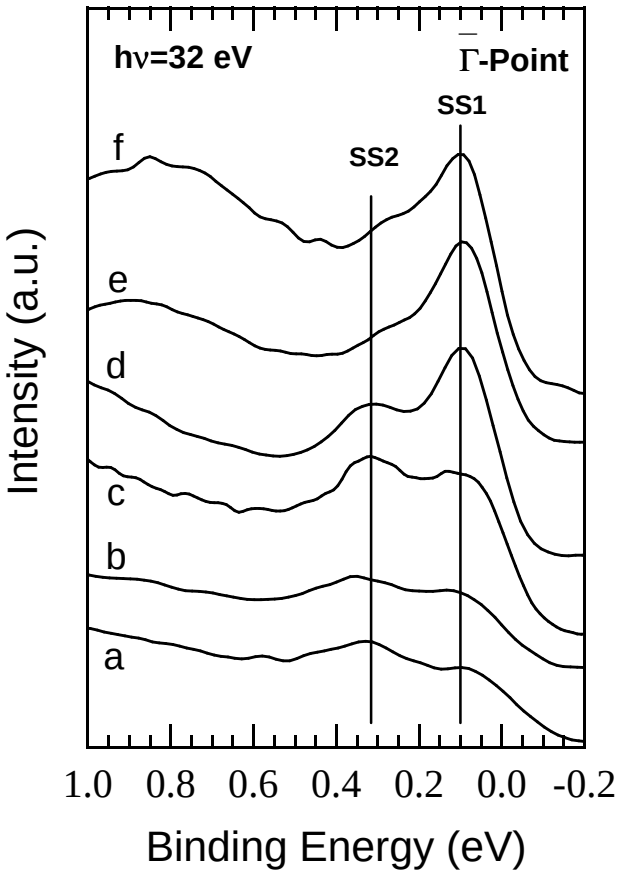
hν=32 eV
Γ̄-Point
SS1
SS2
f
e
d
c
b
a
Intensity (a.u.)
1.0 0.8 0.6 0.4 0.2 0.0 -0.2
Binding Energy (eV)

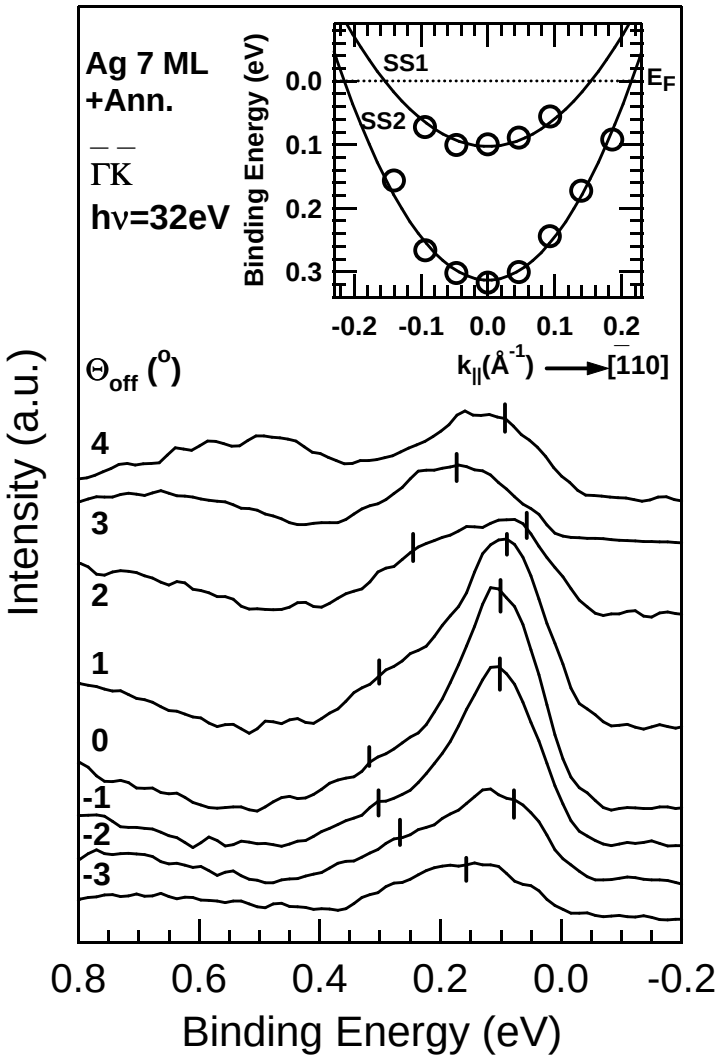
Ag 7 ML
+Ann.
$\bar{\Gamma}\bar{K}$
hν=32eV
Binding Energy (eV)
0.0
0.1
0.2
0.3
SS1
SS2
E_F
-0.2 -0.1 0.0 0.1 0.2
$k_{||}(Å^{-1})$ → $\bar{[110]}$
Θ_{off} (°)
4
3
2
1
0
-1
-2
-3
Intensity (a.u.)
0.8 0.6 0.4 0.2 0.0 -0.2
Binding Energy (eV)

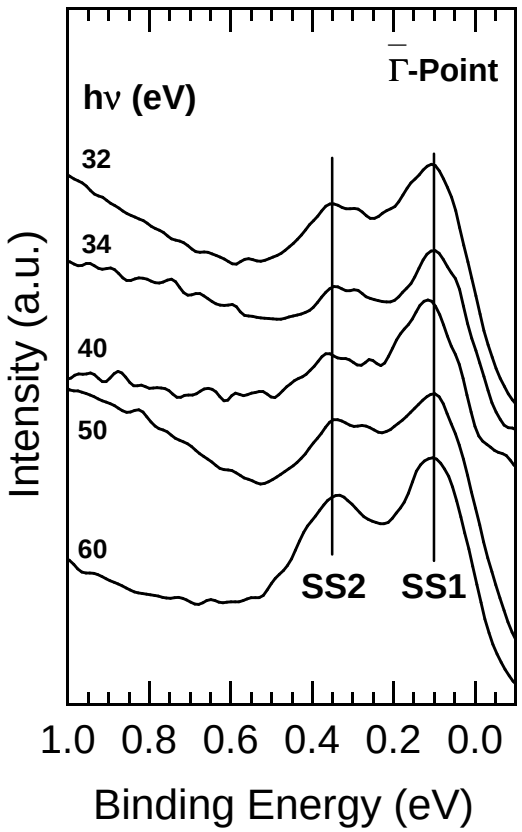
$\bar{\Gamma}$-Point
hν (eV)
32
34
40
50
60
SS2
SS1
Intensity (a.u.)
1.0 0.8 0.6 0.4 0.2 0.0
Binding Energy (eV)

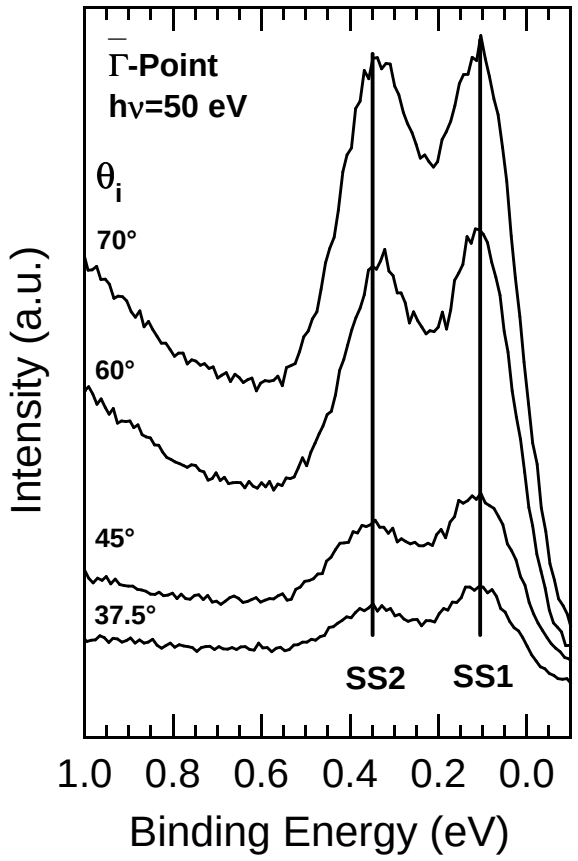
$\bar{\Gamma}$-Point
hν=50 eV
θi
70°
60°
45°
37.5°
SS2
SS1
Intensity (a.u.)
1.0
0.8
0.6
0.4
0.2
0.0
Binding Energy (eV)

This figure "Figure7.jpg" is available in "jpg" format from:

http://arXiv.org/ps/cond-mat/0104189v1

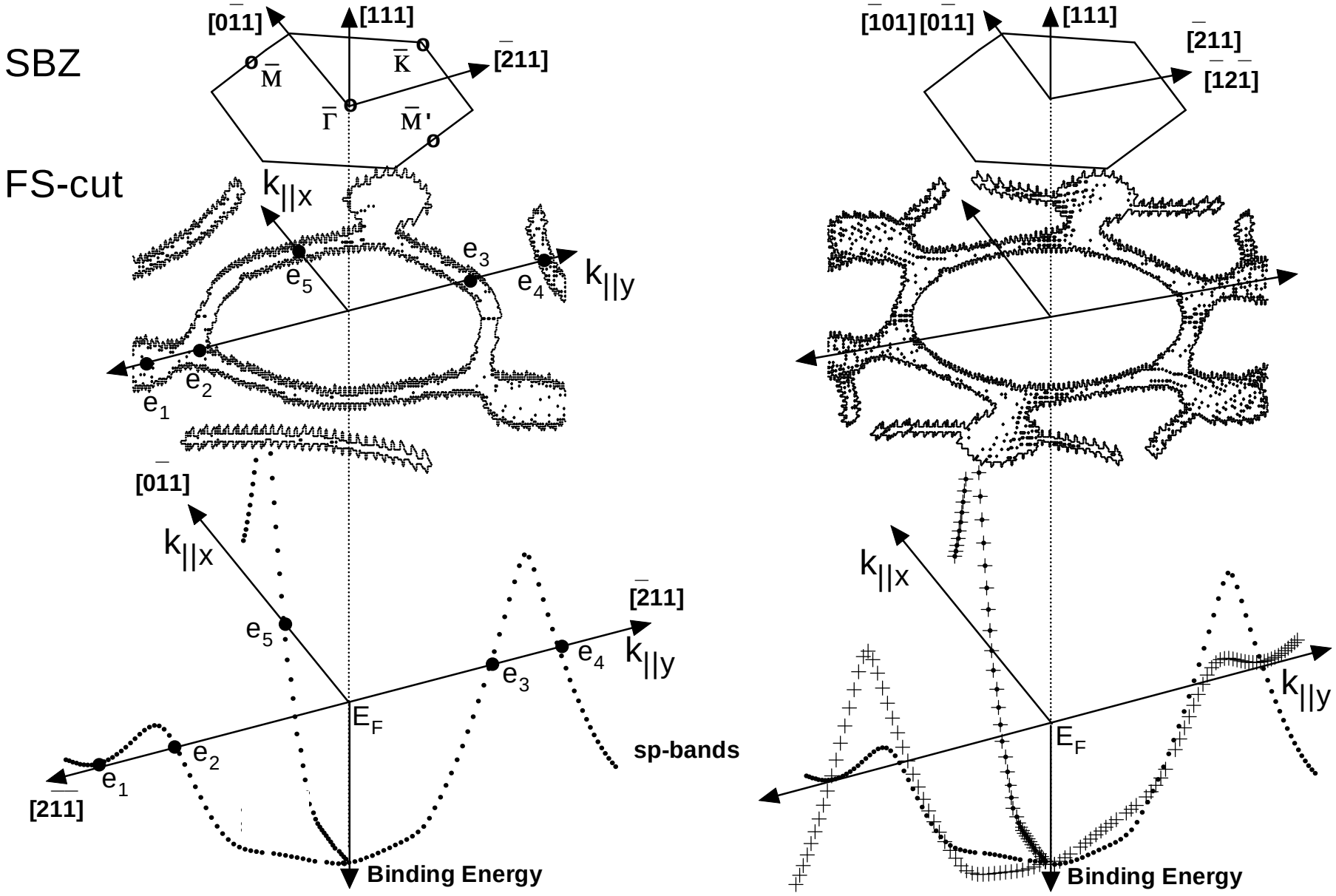
SBZ
FS-cut
[0$\bar{1}$1]
[111]
[$\bar{2}$11]
$\bar{M}$
$\bar{K}$
$\bar{\Gamma}$
$\bar{M}$'
$k_{||x}$
$k_{||y}$
e_1
e_2
e_3
e_4
e_5
E_F
sp-bands
Binding Energy
[$\bar{1}$01]
[$\bar{1}$21]